Archives of Materials Science and Engineering

Volume 55
Issue 2
June 2012
Pages 62-69

International Scientific Journal
published monthly by the
World Academy of Materials
and Manufacturing Engineering

The influence of heat treatment on structure, mechanical properties and corrosion resistance of steel X10CrNi18-8

M. Kciuk*, A. Kurc-Lisiecka

Institute of Engineering Materials and Biomaterials, Silesian University of Technology,
ul. Konarskiego 18a, 44-100 Gliwice, Poland
* Corresponding e-mail address: monika.kciuk@polsl.pl

Received 03.04.2012; published in revised form 01.06.2012

ABSTRACT

Purpose: The aim of the paper is to investigate the influence of the heat treatment on the structure, mechanical properties and corrosion resistance of the steel X10CrNi18-8.

Design/methodology/approach: The investigated steel was solution heat treated at temperature 1050°C with water cooling and it was analysed the susceptibility to intergranular corrosion at temperature 700°C. Structures were investigated using light microscopy. The examinations of the mechanical properties were conducted on ZWICK 100N5A. Hardness measurements were made by Vickers method r. The investigations of the precipitation process were done by X-ray diffraction phase analysis. Corrosion resistance of investigated steel was examined using potentiodynamic methods.

Findings: The structure of analysed steel in as-cast conditions consist of austenitic microstructure with numerous slip bands in areas with deformation martensite α'. The examined steel after solution heat treatment followed by water-cooling has the structure of austenite with a small amount slip bands. Ageing at 700°C caused precipitation of many chromium carbides on the grain boundaries and inside the grain. The best mechanical properties (UTS=1327 MPa, $YS_{0.2}$=1287 MPa, 392 HV) has steel as-cast conditions. It was also found that the investigated steel show poor corrosion resistance in 3.5% NaCl solution. Fractographic analyses of the samples after corrosion tests permitted to define the kind and degree of corrosion damage.

Research limitations/implications: To investigate in more detail the corrosion behaviour 18-8 austenitic steels, the investigations should include immersion tests and an analysis of corrosion products.

Practical implications: The obtained results can be used for searching the appropriate way of improving the corrosion resistance of a special group of steels.

Originality/value: The relationship between the heat treatment, structure, mechanical properties and corrosion resistance of X10CrNi18-8 steel was specified.

Keywords: Heat treatment; Structure; Mechanical properties; Corrosion resistance

Reference to this paper should be given in the following way:

M. Kciuk, A. Kurc-Lisiecka, The influence of heat treatment on structure, mechanical properties and corrosion resistance of steel X10CrNi18-8, Archives of Materials Science and Engineering 55/2 (2012) 62-69.

PROPERTIES

1. Introduction

Austenitic stainless steel have attracted increasing attention over the past few years due to fine structural control for tailoring engineering properties. These steels are widely used as a materials for applications requiring excellent resistance to corrosion in combination with good mechanical properties [1].

The microstructure of the austenitic stainless steel is composed of the metastable soft parent face-centered-cubic austenite (γ) phase, and the steels generally have low and stacking fault energy (SFE), however the SFE must play also an important role in determining the austenite stability, since it controls the formation of the shear bands, and thus the formation of nucleation sites of the α' - martensite phase.

It is well known that the SFE is strongly dependent on the chemical composition and temperature [2,3].

The deformation process of metastable austenite phase involves the formation of strain-induced - ε and α' martensite phase. The transformation sequence γ→ε→α' was proposed by some authors for AISI 304 and 316 deformed by tension and rolling but the direct transformation γ→α' through dislocations reactions was found to be possible [4,5].

At the early stages of deformation, shear bands consisting of stacking fault bundles and deformation twins are formed, promoted by the low SFE of the steels.

The ε-martensite phase is hcp, paramagnetic and is formed by overlapping stacking faults, and therefore, it is finely dispersed and its structure is heavily faulted. The crystal structure of α'-martensite is body-centered cubic, and it is nucleated at the intersections of shear bands [6-10].

It is known that martensitic transformation, like other changes, derived from shear stress, which cause microscopic wave propagations on the surface of the material and an increase in volume resulting in residual tensions [10-13].

Although austenitic stainless steels possess excellent resistance to general corrosion, they are susceptible to the localized corrosive attacks, such as pitting corrosion, intergranular corrosion and stress corrosion cracking (SCC), in chloridecontaining environments [14,15].

The high corrosion resistance of austenitic stainless steels in most atmospheric and aqueous environments is due to passivation by a thin (~2nm) layer of chromium oxide.

Pitting is simply a breakdown of the chromium oxide layer followed by localised corrosion that produces pits, which may cause perforation of a vessel or pipework (Fig. 1).

The anodic dissolution of the steel leads to introduction of positive metal ions (M^+) in solution, which causes migration of Cl^- ions. In turn, metal chloride reacts with water according to the reactions [6]:

$$M + Cl^- + H_2O \rightarrow MOH + H^+ + Cl^- \quad (1)$$

This causes the pH decrease. The cathodic reaction, on the surface near the pit follows:

$$O_2 + 2H_2O \rightarrow MOH + 4OH^- \quad (2)$$

Pitting is mainly associated with microscopic heterogeneities in a surface rather than macroscopic physical features of a component. Wet and humid environments containing chloride ions can cause pitting corrosion and crevice corrosion of austenitic stainless steel components.

Chloride ions are known to be potent corrosion enhancers and localized adsorption of chloride ions can act as prenuclei for pitting. Pits can also nucleate at carbides, grain boundaries and other material inhomogenities on the metal surface.

The presence of moisture in the environment can facilitate the electrolityc path for the chloride ions.

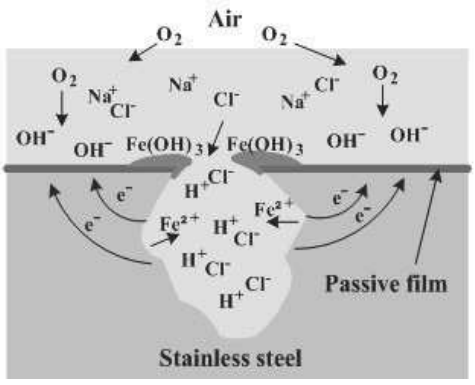

Fig. 1. Pitting corrosion of stainless steel [16]

Pits act as sites for the nucleation of stress corrosion cracks, which can lead to catastrophic failures. SCC occurs as a result of the synergistic action of three factors [17]:

- susceptible microstructure,
- corrosive environment,
- tensile stresses present.

Depending on the microstructure of the material exposed and the nature of environment, the cracking may be intergranular i.e. passing through the grain boundaries or transgranular i.e. passing through the grain matrix or it may be a mixed mode (transgranular and intergranular) of SCC.

The phenomenon of intergranular corrosion (IGC) has found much attention in literature. Grain boundaries and the neighbored areas of the grains normally are chemically different compared to the bulk grains themselves [18,19].

When austenitic steels have been exposed for a period of time in the range of approximately 425 to 850°C, or when the steel has been heated to higher temperatures and allowed to cool through that temperature range at a relatively slow rate (such as occurs after welding or air cooling after annealing) new phases can be formed at the grain boundaries such as metal carbides [20].

Formation of these carbide particles in the grain boundaries depletes the surrounding metal of chromium and reduces its corrosion resistance, allowing the steel to corrode preferentially along the grain boundaries.

Many studies to reduce the risk of IGC have been focused on the practices to prevent the precipitation of Cr-carbides and Cr-carbonitrides along the grain boundaries in stainless steels [21].

The effective practical methods to prevent IGC are decreasing the C or N content and adding stabilizers such as Ti and Nb. Titanium and niobium each have much higher affinities for carbon than chromium and therefore titanium carbides, niobium carbides and tantalum carbides form instead of chromium carbides, leaving the chromium in solution and ensuring full corrosion resistance [22].

2. Experimental procedure

The experimental research was carried out on austenitic steel X10CrNi18-8 with a chemical composition presented in Table 1. The material used for the investigations was delivered in the form of wire with a diameter of about 2.5 mm and was solution heat treated at 1050°C and sensitized at 700°C. This type of steels have an adequate combination of mechanical properties and resistance to corrosion, they are used in a wide variety of industries, such as the food, transport, nuclear and petrochemical industries.

Table 1.
Chemical composition of the investigated steel

Mass contents, (%)						
C	Cr	Ni	S	P	Si	Mn
0.081	18.21	8.33	0.006	0.042	0.390	0.919

The static tensile tests were made on the universal strength machine Zwick 100N5A at room temperature accordantly to PN-EN 10002-1:2004 standard.

The hardness tests were performed using Vickers hardness test method (HV). The measurements were obtained on the FM 700 Future -Tech hardness tester, equipped with electronic sensor that allows the direct readout of the hardness values. In this technique measurements were made at 50 N load, eliminating influence of the substrate on the measurements results.

Metallographic examinations of the material structure in the delivery state and after heat treatment were made on the light microscopy with magnification to 1000x.

The X-ray tests were realized with the use of Dron 2.0 diffractometer equipped with the lamp of the cobalt anode of 40 kV voltage and 20 mA filament current was used. Diffraction tests were carried out in the 2θ angle range from 20 to 90° (measurement step 0.05°). Pulse counting time was 4s. The obtained diffractions patterns were analyzed applying the PCPDFWIN program.

Corrosion resistance of investigated steel was examined using potentiodynamic methods. Corrosion tests were carried out in 3.5% solution of NaCl. Temperature of the solution during the test was equal 23ºC ± 1ºC. Specimens were cleaned in 95.6% ethanol before starting the analysis.

Tests were initiated from determination of E_{ocp} open circuit potential and then anodic polarization curves with a rate of potential changes of 1 mV/s in the anodic direction were registered. After the current density being equal 1 mA/cm^2 was achieved, the direction of polarization has been changed. In such way, the return curve was registered.

According to registered curves, chemical quantities describing corrosion resistance were determined: pitting potential E_b (mV), repassivation potential E_{cp} (mV) - if occurred, polarization resistance R_p (kΩ·cm^2) and corrosion current i_{cor} (A/cm^2). In order to calculate the corrosion current, the Stern-Geary equation) was used [23,24]:

$$R_p = \frac{b_k \cdot b_a}{2.3 \cdot i_{cor}(b_a + b_k)} \tag{3}$$

where:
b_k - the slope coefficient of the cathodic Tafel line, b_a - the slope coefficient of the anodic Tafel line, i_{cor} - the corrosion current density [mA/cm^2], R_p - the polarization resistance [kΩ/cm^2].

Fractographic analyses of surface of specimens after corrosion tests were conducted using DSM 940 Digital Scanning Microscope, with 12nm of resolving power and 15 kV of accelerating voltage, supplied by OPTON Company.

3. Results and discussion

Metallographic microscopic research that was carried out permitted to observe microstructure of the samples in delivery state and after heat treatment. Specimens taken from the delivered material reveal austenite microstructure with annealing twins and numerous slip bans inside the grains of γ phase.

a)

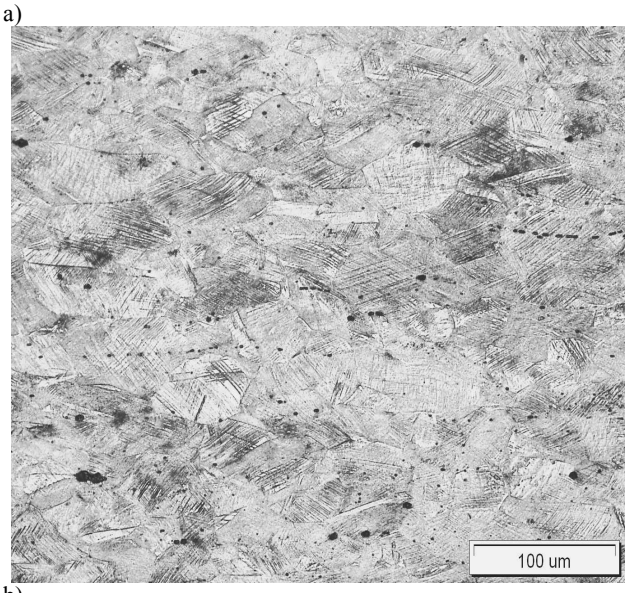

b)

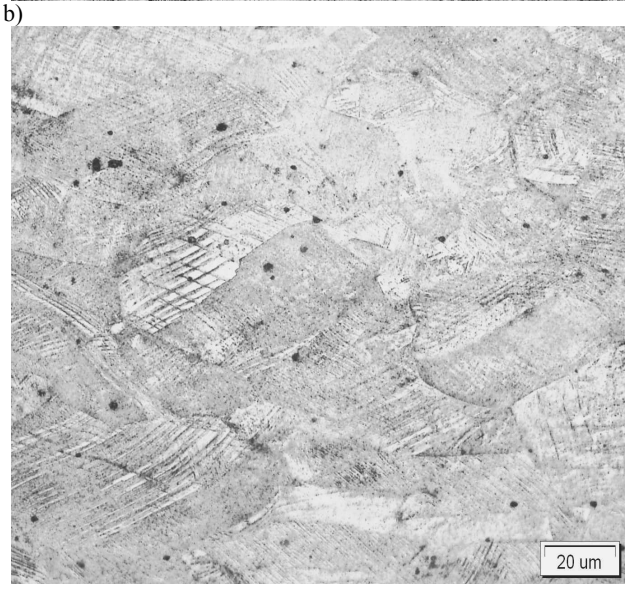

Fig. 2. Structure of the investigated steel in the delivery state 400x (a); 1000x (b)

In the delivery state of investigated steel were observed the areas of martensite phase α'. Austenite grains characterized with some deformation (Fig. 2).

Metallographic observations of structure after heat treatment at temperature 700°C show that the chromium and carbon in the steel combine to form particles along the grain boundaries throughout the steel.

Formation of these carbide particles in the grain boundaries depletes the surrounding metal of chromium and reduces its corrosion resistance, allowing the steel to corrode preferentially along the grain boundaries. Steel in this condition is said to be "sensitised" (Fig. 3).

As shown in Fig. 4 the microstructure of the samples annealed at 1050°C characterized by the austenitic single-phase structure.

The X-ray investigation allowed to identify the phase composition of analyzed steel in the delivery state and after heat treatment. The results obtained for samples in the delivery state are presented in Fig. 5.

The results of diffraction patterns of phase analysis revealed the presence of austenite (γ-phase) and α'-martensite. On diffraction patterns of steel in the delivered state disclosed diffraction lines coming from planes (111), (200), (220) austenite phase and (110) α'-martensite phase.

a) b)

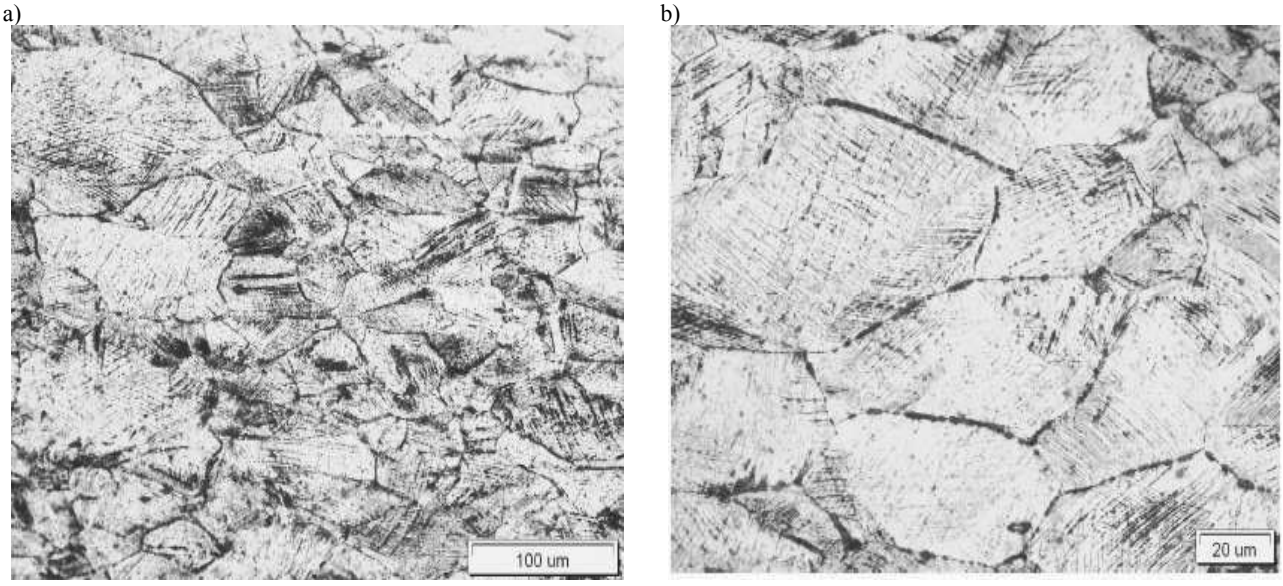

Fig. 3. Structure of the steel annealed at temperature 700°C, 400x (a); 1000x (b)

a) b)

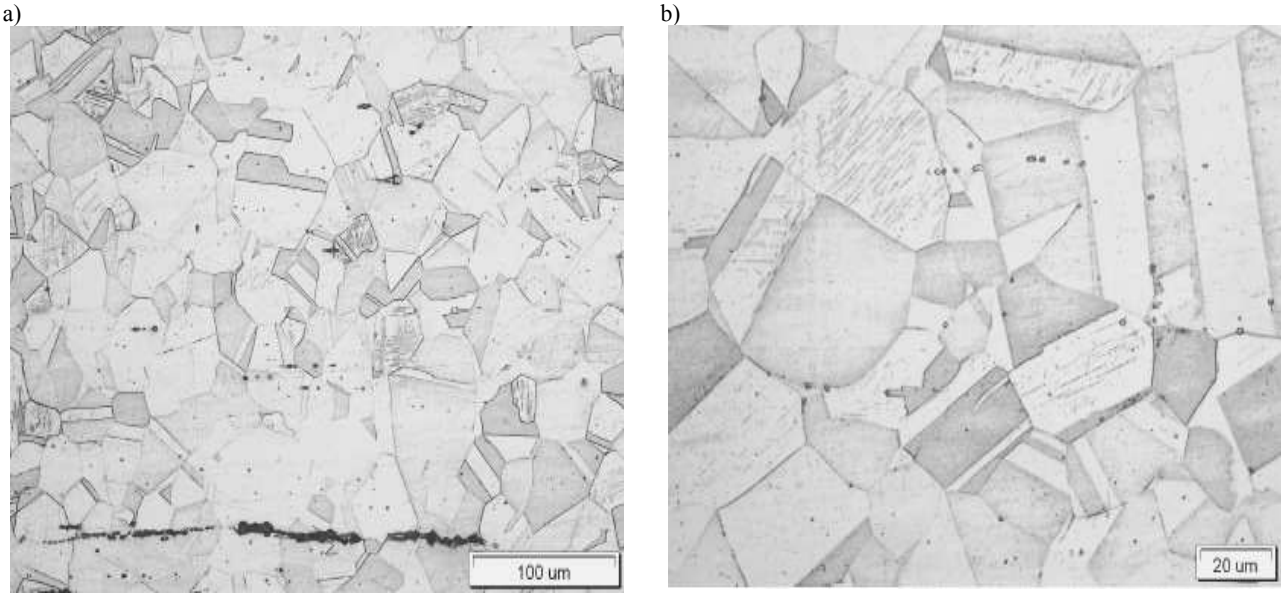

Fig. 4. Structure of the steel annealed at temperature 1050°C, 400x (a); 1000x (b)

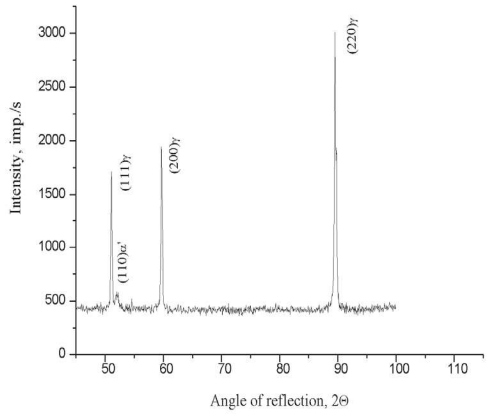

Fig. 5. X-ray diffraction pattern of X10CrNi18-8 in delivery state

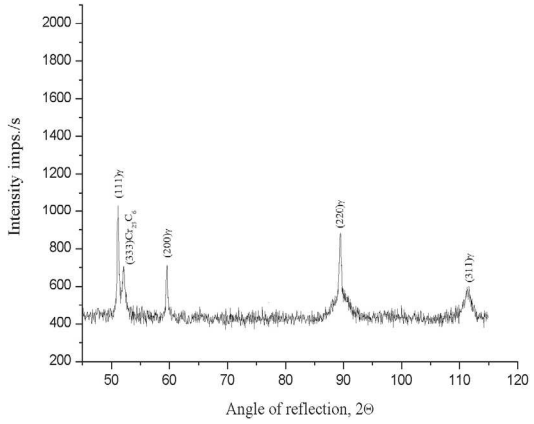

Fig. 6. X-ray diffraction pattern of X10CrNi18-8 after heat treatment at 700°C

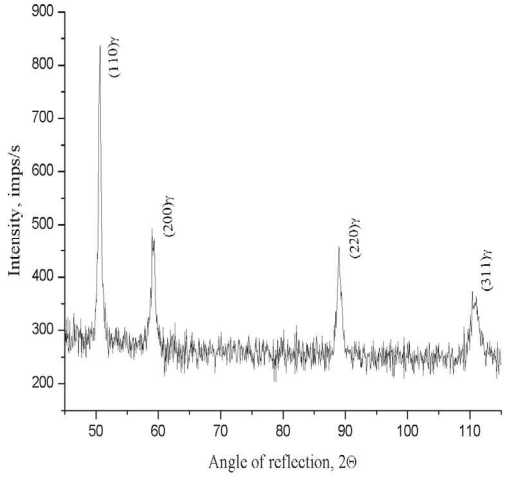

Fig. 7. X-ray diffraction pattern of X10CrNi18-8 after heat treatment at 1050°C

After sensitization (Fig. 6), the XRD pattern is typical of austenite-phase, the peaks of which appear at 2θ= 50.892; 59.599; 89.557; 111.577 and lines of chromium carbides at 2θ =51.994. The intensity of chromium carbides was determine by the maximum intensity of γ-phase

Pure austenitic structure after heat treatment at 1050°C was confirmed by X-ray diffraction. As shown in Fig. 7 the investigated sample exhibits only austenite diffraction lines.

The results of the mechanical properties of X10CrNi18-8 steel are presented on the Fig. 8. On the basis of the realized tensile tests the tensile strength UTS and yield point $YS_{0.2}$ were determined, additionally the measurements of the hardness were carried out. The tensile strength of the investigated steel in the delivery state is about 1327 MPa, the yield point is about 1287 MPa, the Vickers hardness is about 392 HV5.

In samples after heat treatment at 700°C hardness and strength properties of the examined steel decreases slightly. The value of hardness is on the level 375 HV5 while the tensile strength obtained value 1158 MPa the yield point is about 1056 MPa.

With the increasing of temperature during solution treatment at 1050°C it was noticed rapid decrease of all the mechanical properties of analyzed steel (UTS=670 MPa, $YS_{0.2}$= 360 MPa and HV5= 203).

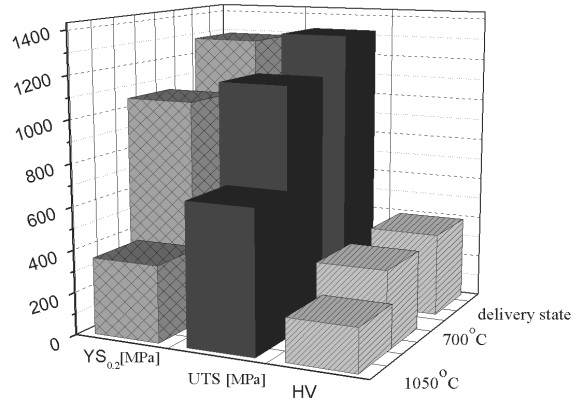

Fig. 8. Changes of the mechanical properties in the investigated steel

Electrochemical studies showed different resistance to pitting corrosion of steel specimens, depending on the heat treatment.

Performed electrochemical analysis revealed that the open circuit potential for all the samples in the delivery state established itself after 40 min. The course of changes of current density in a function of potential for the samples investigated in 3.5% NaCl solution is presented in Fig. 9. The value of corrosion potential E_{cor} was equal -524 mV and the density of corrosion current i_{cor} determined basing on the Stern-Geary equation was equal 0.042 mA/cm^2.

In specimens after heat treatment at temperature 700°C it was noticed the increase of the current density, which was in the range 0.13-0.15 mA/cm^2 (Fig. 10). This is due to the precipitation of chromium carbides at boundaries and within grains, which decrease the Cr content in the grain boundaries, making steel susceptible to corrosion attack in aggressive environments chlorides.

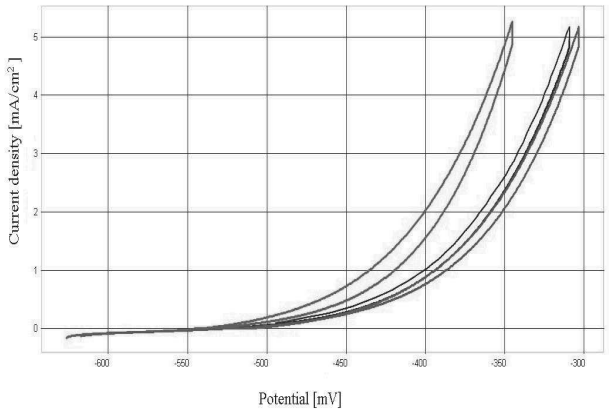

Fig. 9. Anodic polarization curves of X10CrNi18-8 steel in delivery state

The best corrosion resistance to pitting corrosion was indicated in samples after solutioning at 1050°C (Fig. 11). Corrosion current value was equal 0.025 mA/cm^2. The value of corrosion potential E_{cor} was ranged -458 - -482 mV.

Fractographic analyses of sample surface put to corrosion tests allowed to evaluate the type and the degree of corrosion damages.

The study showed that the samples in initial state and after heat treatment showed the heterogeneous nature of corrosion products and intensity of corrosion damage.

Fractographic observations of the steel X10CrNi18-8 in delivery state samples showed that the surface of the examined samples was subjected to the greatest corrosion attack in places where has been probably the local breakdown of the passivation oxide layer in presence of aggressive anions of the environment.

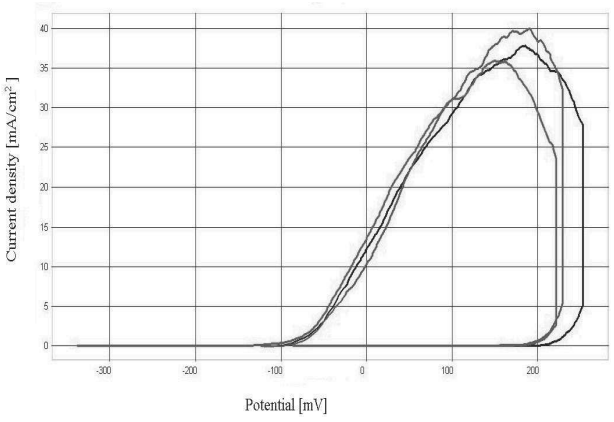

Fig. 10. Anodic polarization curves of X10CrNi18-8 steel after sensitization

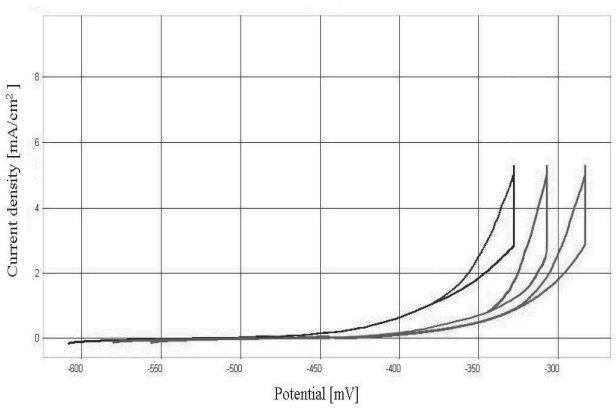

Fig. 11. Anodic polarization curves of X10CrNi18-8 steel after solutioning at temperature 1050°C

a) b)

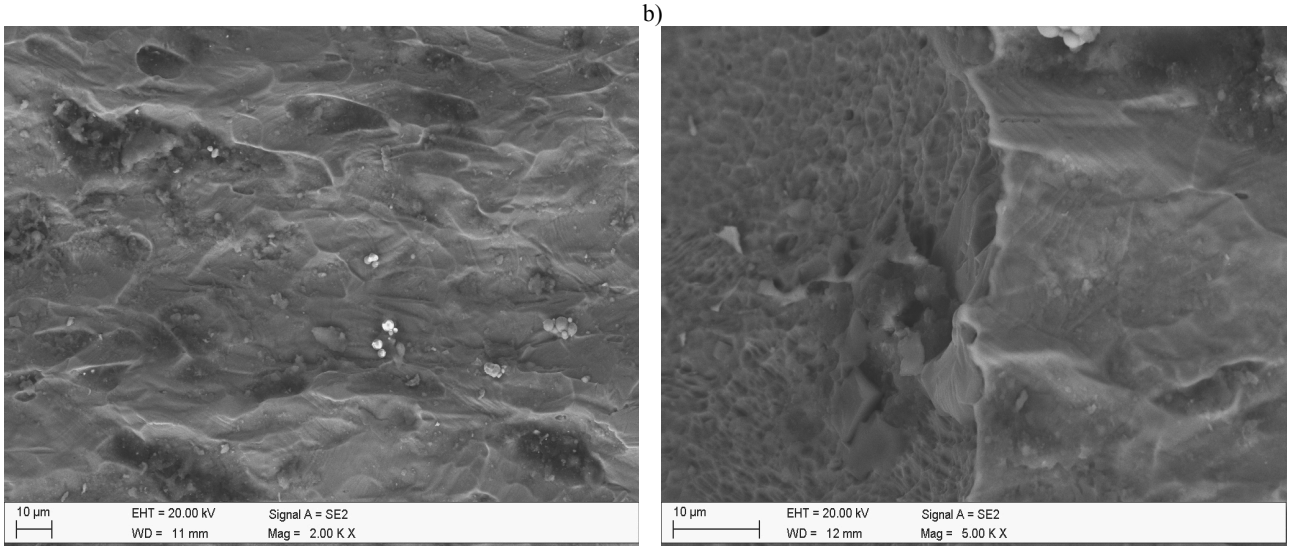

Fig. 12. Corrosion pits and the partially cracked surface layer of the specimen in delivery state; 2000x (a); 5000x (b)

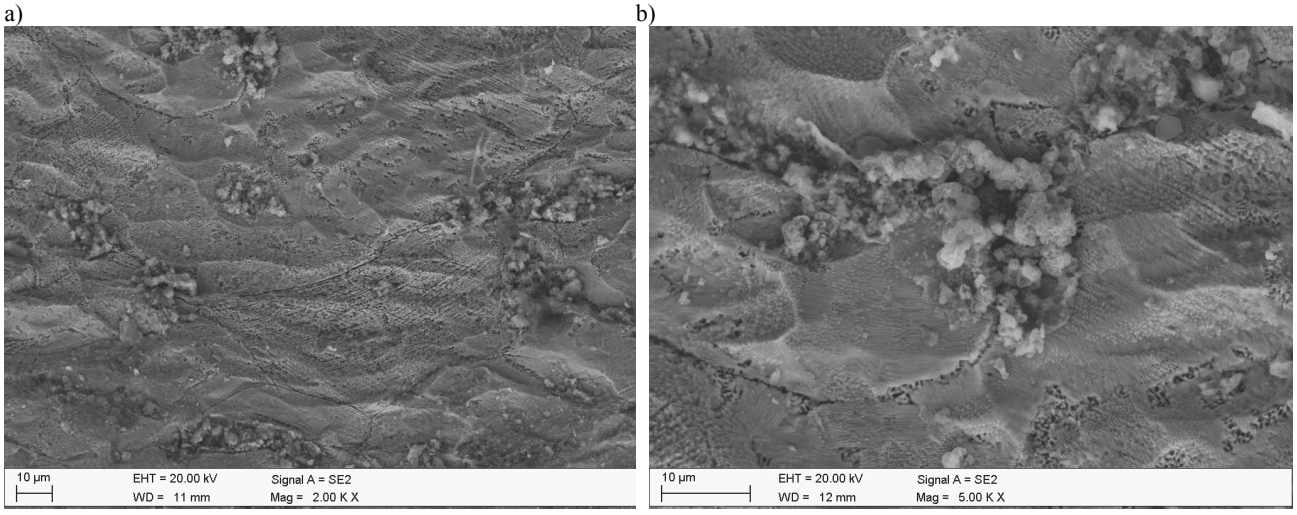

Fig. 13. The surface of the sensitized samples of X10CrNi18-8 steel after corrosion tests in 3.5% NaCl; 2000x (a); 5000x (b)

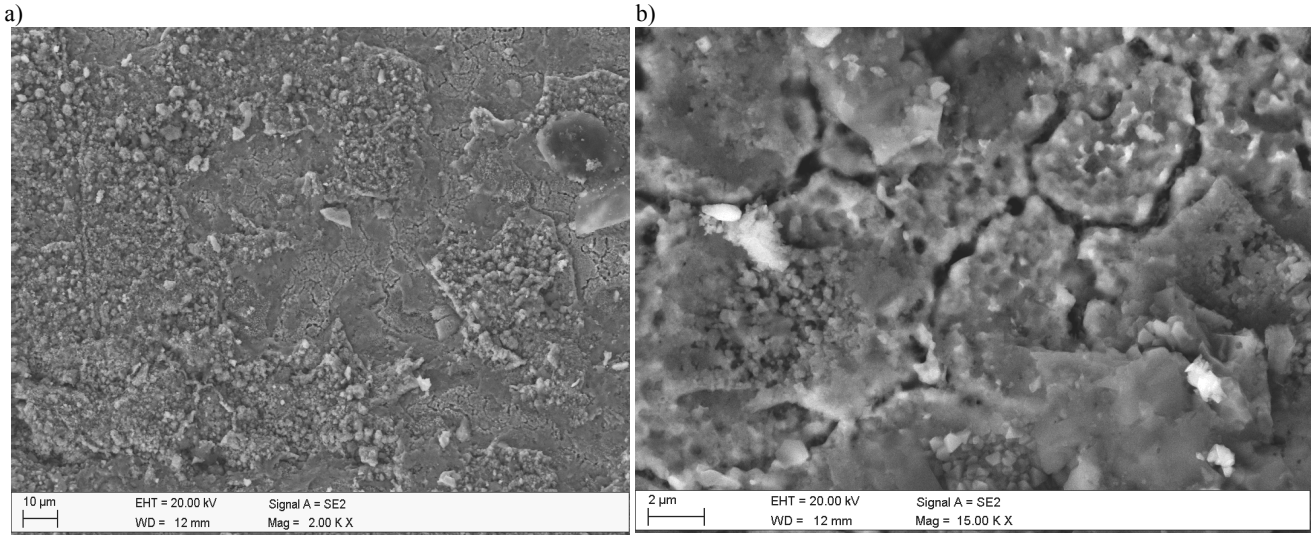

Fig. 14. The surface of X10CrNi18-8 steel in solutioning state and after corrosion investigations in 3.5% NaCl, 2000x (a); 15000 (b)

The corrosion rate is increased by the fact that even more aggressive environment is produced by the corrosion reaction itself. As a result of observation it was noticed the pits occurrence of various sizes and initiating the process of scaling of the sample surface (Fig. 12).

The morphology of the samples after sensitization to intergranular corrosion showed the presence of the large oval pits and the formation on the surface corrosion products as scales in different sizes (Fig. 13). It was also found that in the samples after sensitization, in places where chromium-rich $M_{23}C_6$ carbides were formed occurred a diminished ability to formation a passive film, for this reason the grain boundaries corrode preferentially.

In the structure after solutioning was revealed scalling process of the surface and cracked surface layer of the specimen (Fig. 14).

4. Conclusions

Metallographic investigations of samples in delivery state revealed austenite microstructure with annealing twins and numerous slip bans inside the grains of γ phase.

Were also observed the areas of martensite phase α' ensuring the high value of tensile strength UTS = 1327 MPa, yield strength $YS_{0.2}$ = 1287 MPa and hardness HV5 = 392.

Sensitization of the analyzed steel leads to formation of chromium carbides. A slight decrease of strength parameters it was noticed. Tensile strength is at a level of 1158 MPa, yield strength was 1056 MPa, while the HV5 was 372.

After solutioning samples were characterized by the austenitic single-phase structure and it was noticed rapid decrease of all the

mechanical properties of analyzed steel (UTS =670 MPa, $YS_{0,2}$ = 360 MPa and HV5= 203).

The lowest corrosion resistance showed sensitized samples, which is related to the precipitation of the carbides chromium at the grain boundaries. The highest corrosion resistance has been established in samples after sotutioning at temperature 1050°C.

Observations of the samples surface after corrosion tests showed numerous corrosion damages. Conducted fractographic analyses of samples after corrosion tests revealed corrosion products on their surface in a form of pits with diversified size. Damaging of a superficial layer has occurred around the pits.

Moreover, cracked passivation layer allowing further penetration of the corrosive medium.

References

[1] M. Karimi, A. Najafizadeh, A. Kermanpur, M. Eskandari, Effect of martensite to austenite reversion on the formation of nano/submicron grained AISI 301 stainless steel, Materials Charakterization 60 (2009) 1220-1223.

[2] J. Talonen, H. Hänninen, Formation of shear bands and strain-induced martensite during plastic deformation of metastable austenitic stainless steels, Acta materialia 55 (2007) 6108-6118.

[3] A. Kurc, M. Kciuk, M. Basiaga, Influence of cold rolling on the corrosion resistance of austenitic steel, Journal of Achievements in Materials and Manufacturing Engineering 38/2 (2010) 154-162.

[4] K. Pałka, A. Weroński, K. Zalewski, Mechanical properties and corrosion resistance of burnished X5CrNi18-9 stainless steel, Journal of Achievements in Materials and Manufacturing Engineering 16 (2006) 57-62.

[5] H.F. Gomes de Abreu, S. Santana de Carvalho, P. de Lima Neto, R. Pires dos santos, V. Nogueira Freire, P. M. de Oliveira Silva, S. Souto Maior Tavares, Deformation induced martensite in an AISI 301LN stainless Steel: characterization and Influence on pitting corrosion resistance, Materials Research 10/4 (2007) 359-366.

[6] W. Ozgowicz, A. Kurc, M. Kciuk, Effect of deformation-induced martensite on the microstructure, mechanical properties and corrosion resistance of X5CrNi18-8 stainless steel, Archives of Materials Science and Engineering 43/1 (2010) 42-53.

[7] W. Ozgowicz, E. Kalinowska-Ozgowicz, A. Kurc, Influence of plastic deformation on structure and mechanical properties of stainless steel type X5CrNi18-10, Journal of Achievements in Materials and Manufacturing Engineering 32/1 (2008) 37-40.

[8] Xu Chunchun, Hu Gang, Effect of deformation-induced martensite on pit propagation behavior of 304 stainless steel, Anti-Corrosion Methods and Materials 51 (2004) 381-388.

[9] A. Pardo, M.C. Merino, A.E. Coy, R. Arrabal, F. Viejo, A. M'hich, Corrosion behaviour of AISI 304 stainless steels with Cu coatings in H_2SO_4, Applied Surface Science 253 (2007) 9164-9176.

[10] P.M. de O. Silva, H.F.G. de Abreu, V. H.C. de Albuquerque, P. de Lima Neto, J.M.R.S. Tavares, Cold deformation effect on the microstructures and mechanical properties of AISI 301LN and 316L stainless steels, Materials and Design 32 (2011) 605-614.

[11] E. Swallow, H.KD.H. Bhadeshia, High resolution observations of displacements caused by bainitic transformation. Material Science Technology 12 (1996) 121-125.

[12] YD. Wang, RL. Peng, XL. Wang, RL. McGreevya, Grain-orientation-dependent residual stresses and the effect of annealing in cold-rolled stainless steel. Acta Materialia 50 (2002) 1717-1734.

[13] A. Bahadur, BR. Kumar, SG. Chowdhury, Evaluation of changes in X-ray constants and residual stress as a function of cold rolling of austenitic steels, Material Science Technology 20/3 (2004) 387-392.

[14] B.T. Lu, Z.K. Chen, J.L. Luo, B.M. Patchett, Z.H. Xu, Pitting and stress corrosion cracking behavior in welded austenitic stainless steel, Electrochimica Acta 50 (2005) 1391-1403.

[15] S. Ningshen, U. Kamachi Mudali, Pitting and Intergranular Corrosion Resistance of AISI Type 301LN Stainless Steels Journal of Materials Engineering and Performance 19/2 (2010) 274-281.

[16] http://www.substech.com/dokuwiki/doku.php?id=pitting_corrosion

[17] S. Ghosh, V. Rana, V. Kain, V. Mittal, S.K. Baveja, Role of residual stresses induced by industrial fabrication on stress corrosioncracking susceptibility of austenitic stainless steel, Materials and Design 32 (2011) 3823-3831.

[18] S.M. Bruemmer, Grain boundary chemistry and intergranular failure of austenitic stainless steels, Materials Science Forum 46 (1989) 309-334.

[19] P. Kritzer Corrosion in high-temperature and supercritical water and aqueous solutions, Journal of Supercritical Fluids 29 (2004) 1-29.

[20] L.W. Tsay a, Y.-F. Liua a, R.-T. Huanga, R.-C. Kuo, The effect of sensitization on the hydrogen-enhanced fatigue crack growth of two austenitic stainless steels, Corrosion Science 50 (2008) 1360-1367.

[21] J.K. Kim, Y.H. Kim, B. H. Lee, K. Y. Kim, New findings on intergranular corrosion mechanism of stabilized stainless steels, Electrochimica Acta 56 (2011) 1701-1710.

[22] J.K. Kim, Y.H. Kim, K. Y. Kim, Influence of Cr, C and Ni on intergranular segregation and precipitation in Ti-stabilized tainless steels, Scripta Materialia 63 (2010) 449-451.

[23] J. Baszkiewicz, M. Kamiński, Fundamentals of materials corrosion, The Warsaw University of Technology Publishers, Warsaw, 1997 (in Polish).

[24] M. Opiela, A. Grajcar, W. Krukiewicz, Corrosion behaviour of Fe-Mn-Si-Al, Journal of Achievements in Materials and Manufacturing Engineering 33/2 (2009) 159-165.